# Consequences of an adjusted slip layer thickness for the hardened properties of UHPC

VAN DER PUTTEN Jolien[1,a *], LESAGE Karel[1,b] and DE SCHUTTER Geert[1,c]

[1]Magnel Laboratory for Concrete Research, Technologiepark-Zwijnaarde 904, 9052 Ghent, Belgium

[a]Jolien.VanDerPutten@UGent.be, [b]Karel.Lesage@UGent.be, [c]Geert.DeSchutter@UGent.be

*corresponding author

**Keywords:** lubrication layer, water absorption, permeability coefficient, UHPC

**Abstract.** The pumpability of a concrete mixture cannot be described by one "single parameter". The mixture composition, the pump equipment, the pumping pressure,… these parameters all affect the pumpability of a mixture and the ability to form a lubrication layer. Especially in case of ultra-high performance concrete (UHPC), where an optimal packing density, a high amount of powders and a low water/binder-ratio are necessary, the formation of that layer is not evident. In this research, the particle mobility is improved by adding an excess amount of paste to a reference UHPC-mixture in order to create a slip layer. As the required slip layer thickness of a pumpable UHPC-mixture is still unknown, different values are taken into account, reaching from 1 to 10 mm. The varying thickness influences the concrete properties in hardened state. One can see that for a thicker lubrication layer, the durability properties decrease due to a higher porosity. The compressive strength is more or less the same comparing the different mixtures.

## Introduction

Concrete pumping is a very common technique that has been widely used to transport fresh concrete on construction sites. Pumping operations are often based on an engineer's experience or on simplified design charts [1]. However, a quantitative prediction such as predictions of pumping height and pressure are necessary to control the total duration of the construction period and the related construction cost [1, 2]. Different investigations [3-5] showed that the dominant factor to facilitate the pipe flow of pumped concrete is the formation of the lubrication layer, also called slip layer. Due to a stress gradient, a redistribution of the particles occurs near the pipe wall. Coarse aggregates move towards the center of the pipe, while the fine materials move towards the pipe wall in order to form an easily deformable lubrication layer. This layer has a lower viscosity, a decreased particle concentration and it will enhance the pumpability of a mixture [4, 6].

However, in case of ultra-high performance concrete (UHPC), the formation of that layer is not that evident. This type of concrete is characterized by an optimal packing density of the aggregates, a high amount of powders and a water/binder-ratio lower than 0.25 in order to achieve a compressive strength higher than 150 MPa. Due to particle interlocking, the mobility of the particles is limited and the formation of the required lubrication layer will be counteracted. To improve the particle mobility, an excess amount of paste is added to a reference UPHC-mixture in order to create a certain lubrication layer. As the required slip layer thickness is still unknown, different values are taken into account, reaching from 1 to 10 mm.

The change in pore structure due to a different mixture design has not only an influence on the pumpability of the mixture, but also on the transport properties and the durability of the material [7]. Regarding the transport properties, the gas permeability coefficient is a parameter giving an indication of the resistance against several kinds of deterioration. Based on the theory of Powers, also an estimation of the capillary porosity is made and its relationship with the gas permeability is investigated. The durability is checked based on a water absorption test. These results are compared with the compressive strength of the mixtures with adjusted slip layer thicknesses.

## Mixture proportions

**Materials.** In this research, basalt is combined with cement, silica fume, quartz flower and quartz sand. Quartz sand (M31) has a density of 2650 kg/m³ and a mean particle size of 370 µm. The chemical composition of the aggregates and the powders can be found in Table 1. CEM I 52.5 N (HSR/LA) has a particle size distribution with a $d_{50}$ of 11.87 µm and a Blaine fineness of 3975 cm²/g. In order to decrease the amount of cement, quartz filler (M400) is used. It has a 99.5 wt.% $SiO_2$, a $N_2$-BET specific surface of 1.9 m²/g and a $d_{50}$ equal to 12 µm. In order to optimize the paste matrix, also silica fume is applied to decrease the porosity. The silica fume is a densified type (DSF) with a $N_2$-BET specific surface equals to 15.51 m²/g and a $d_{50}$ of 12.60 µm. A polycarboxylic ether was used as superplasticizer with a molecular weight of approximately 40000 g/mol and 35% solids. The chemical and mineralogical composition of the powders, used in this research, is given in Table 1. The particle size distribution can be seen in Fig. 1.

**Table 1:** Chemical and mineralogical composition of the mixture components

| **Chemical Composition [%]** | **$SiO_2$** | **$Al_2O_3$** | **$Fe_2O_3$** | **CaO** | **$K_2O$** | **MgO** | **$Na_2O$** | **$SO_3$** | **Alkali** |
|---|---|---|---|---|---|---|---|---|---|
| Basalt (CAB) | 44.58 | 11.50 | 4.30 | 10.77 | 0.65 | 12.98 | 2.11 | - | - |
| Quartz sand | 99.50 | 0.20 | 0.04 | 0.01 | 0.03 | - | - | - | - |
| Cement | 20.90 | 3.64 | 5.19 | 63.68 | 0.63 | 0.77 | 0.17 | 3.03 | - |
| M400 | 99.50 | 0.20 | 0.03 | 0.02 | 0.05 | - | - | - | - |
| DSF | 94.73 | 0.36 | 0.71 | 0.20 | 0.90 | 0.39 | 0.20 | 0.27 | 0.79 |
| **Mineralogical composition [%]** | **$C_3S$** | **$C_2S$** | **$C_3A$** | **$C_4AF$** | | | | | |
| Cement | 59.82 | 14.88 | 0.88 | 15.78 | | | | | |

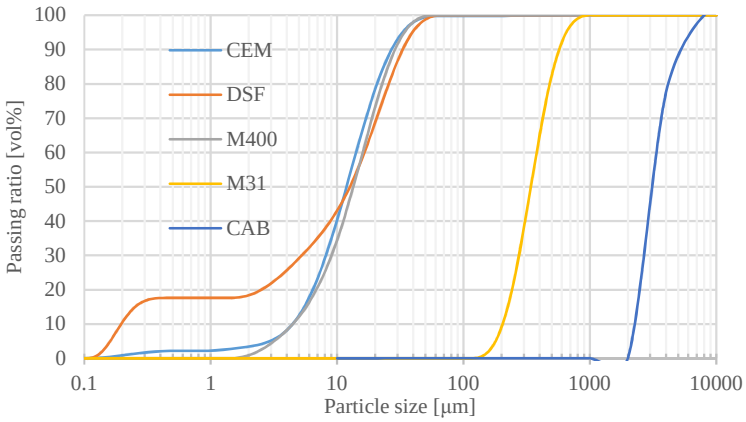


**Fig. 1: Particle size distribution of mixture components**

**Mixture compositions.** The capacity to form and preserve a certain lubrication layer in a mixture is a very important factor. During pumping, shear stress evolves linearly from pipe axis to pipe surface and shear deformation concentrates in this lubrication layer depleted from the coarse aggregates. Based on the shear induced particle migration phenomenon, it can be expected that the extent of the migration, and therefore the lubrication layer thickness shall increase with the reduction in the initial volume of aggregates (or increasing paste volume) [2]. Furthermore, a decrease in workability has been reported with an increase of coarse aggregate fraction [8].

Based on these investigations, it can be expected that the larger the paste content, the easier this lubrication layer will be formed. Therefore, five different mix compositions were defined with a different volume percentage of mortar. The different volume contents in the mixtures are calculated, starting from the reference mixture.

The lubrication layer is assumed to have the same composition as the extracted mortar from the concrete, whereas the bulk material is supposed to consist out of the original concrete mix. Consequently, to form a theoretical slip layer of a certain thickness, extra mortar has to be added in the mix. From this point of view, the reference mix will have no lubrication layer. The different mix compositions are shown in Table 2.

**Table 2:** Concrete composition based on a theoretical slip layer thickness

| **Component [-]** | **ref [kg]** | **1 mm [kg]** | **2 mm [kg]** | **3 mm [kg]** | **10 mm [kg]** |
|---|---|---|---|---|---|
| Cement | 18.96 | 19.31 | 19.54 | 19.77 | 21.24 |
| DSF | 5.94 | 6.05 | 6.12 | 6.19 | 6.66 |
| Sand | 13.02 | 13.26 | 13.42 | 13.57 | 14.59 |
| Basalt 2/4 | 26.10 | 24.88 | 24.09 | 23.30 | 18.18 |
| M400 | 4.74 | 4.83 | 4.89 | 4.94 | 5.31 |
| PCE | 0.81 | 0.83 | 0.83 | 0.84 | 0.91 |
| Water | 3.99 | 4.06 | 4.11 | 4.16 | 4.47 |

## Durability indicator tests and results

**Water absorption.** The water absorption test was, according to NBN B 15-215, determined on 100 mm cubes at 28 days of water curing. Afterwards, the samples were dried in a hot air at 105°C±5°C until constant weight was reached. Eq. 1 was used to calculate the water absorption coefficient W [mass%] of the different mixtures:

$$W = \frac{B - A}{A} \cdot 100 \quad (1)$$

where A is the mass of the oven dried sample [g], B the mass of the surface-dry sample after immersion [g].

Fig. 2 shows the water absorption coefficient of the different mixtures. Water absorption has a direct relationship with the voids, so the water absorption increases as the voids increase. Observing the reference mixture, one notices that the packing density of the coarse aggregates and the powders is very high. Consequently, the amount of voids is very small due to the linear relationship between the packing density and the voids. By decreasing the aggregate volume and increasing the paste, the packing density is reduced and the total amount of voids is higher.

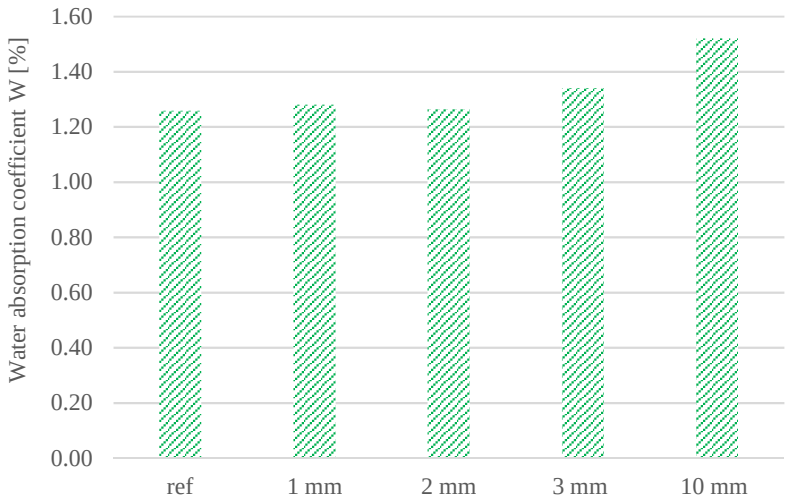


**Fig. 2: Water absorption coefficient**

**Gas permeability of concrete.** The gas permeability is a measure of the flow of gas through a porous material caused by pressure head. It depends on the open porosity prevailing in this material. For this reason, it is important to take into account the moisture content of the concrete since the acting gas pressure in the pores is not sufficient to move the water and the pores will remain blocked, not able to let the gas pass [7].

For each mixture, one prism 400 x 400 x 400 mm³ is made and stored in a climate room at 20 ± 2°C and more than 90% R.H. At the age of 28 days, three cores of 150 mm diameter were drilled for each concrete mixture and from the center of these cores, samples with 50 mm height were taken. Afterwards, the test samples were dried at 105°C to reach a saturation degree of 0%. The test is performed at three different levels of inlet pressures, namely 2, 3 and 4 bar. The test equipment and a detail of a testing cell are shown in Fig. 3. This apparatus can be used for measuring values of the gas permeability in the range of 10-19 to 10-14 m². In order to avoid a change of the pore structure during the applied gas should not react chemically with the concrete. For that reason oxygen is used [7] [9].

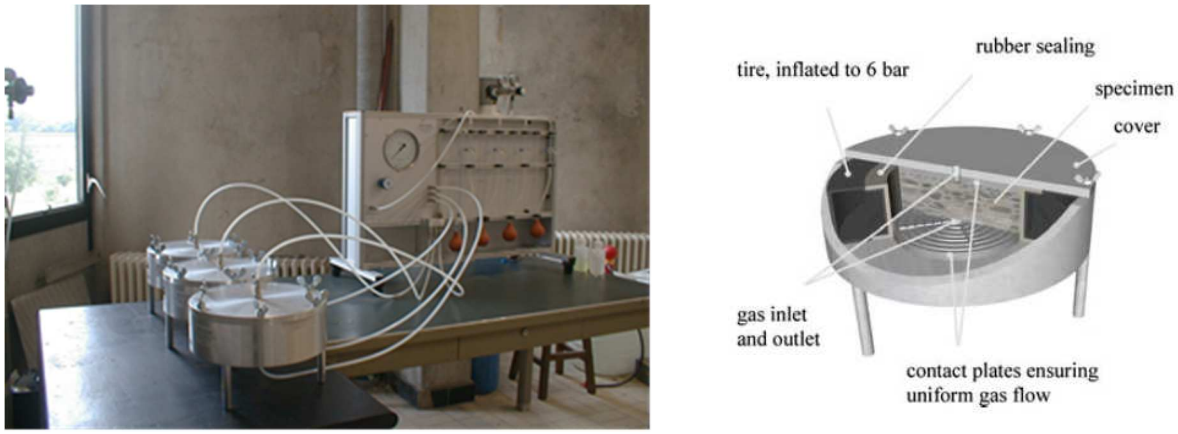


**Fig. 3: Gas permeability equipment and a detail of the testing cell**

The apparent gas permeability $k_{app}$ [m²] can be calculated by means of Eq. 2, based on the Hagen-Poiseuille relationship for laminar flow of a compressible fluid through a porous body with small capillaries under steady-state conditions:

$$k_{app} = \frac{4.04\ P_2\ Q\ L}{A(P_1^2 - P_2^2)} \cdot 10^{-16} \quad (2)$$

with Q the volume flow rate of the fluid measured during the test with a bubble flow meter [ml/s], L the thickness of the specimen in the direction of the flow [m], A the cross-sectional area of the specimen [m²], P1 and P2 the inlet and outlet pressure of oxygen [bar]. This formula is valid for tests performed at 20°C for which the viscosity of oxygen is 2.02 $10^{-5}$ $Nsm^{-2}$.

Fig. 4 shows the change in gas permeability of the different mixture. When the powder content is increased from 988 kg/m³ (reference mixture) to 1107 kg/m³ (10 mm), the gas permeability increases. The C/P, W/C and W/P do not change, but the total amount of paste per m³ increases, making the concrete more porous. This means that there are more holes and the structure is also less denser due to a lower aggregate volume. Consequently, the oxygen can flow more easily through the concrete structure.

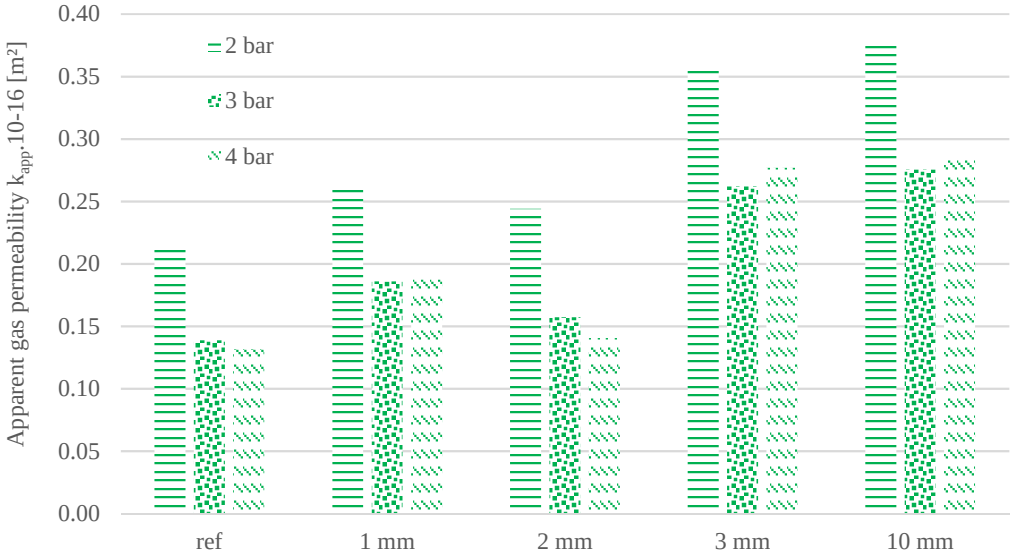


**Fig. 4: Gas permeability coefficient**

**Capillary porosity.** The transport properties of concrete are mainly determined by the capillary pores [10]. In this part of the research it is investigated whether there is a link between the calculated capillary porosity and the gas permeability. The calculation of the capillary pores is based on the Powers' model. Free water is the initial amount of water minus the gel-water and bounded water (Eq. 3):

$V_{cap}$ = capillary pores + free water

= capillary pores + water – gelwater – bounded water

$$= -0.3191 \frac{Ch}{\rho_c} + \frac{1}{\rho_w} (W - 0.3194\ C\ h) \quad (3)$$

With $V_{cap}$ the volume of the capillary pores [m³], C the cement amount [kg], W the initial water amount [kg], h the degree of hydration [-], $\rho_c$ and $\rho_w$ the mass density of respectively cement and water [kg/m³].

$$V_{concrete} = V_{water} + V_{cement} + V_{coarse\ aggregates} + V_{sand}$$
$$= \frac{W}{\rho_w} + \frac{C}{\rho_c} + \frac{A+S+F}{\rho_{agg}} \quad (4)$$

$$\text{Capillary porosity} = \frac{V_{cap}}{V_{concrete}} \quad (5)$$

with $V_{concrete}$ [m³] the volume of concrete, A the amount of coarse aggregates [kg], S the amount of sand [kg], F the amount of filler [kg] and $\rho_{agg}$ the mass density of the aggregate [kg/m³].

From the mix compositions, the W, C, A, S and F are known. The mass densities of the different components are mentioned in the section 'Mixture proportions'. The test specimens are stored until the testing age in a climate room at 20±2°C and at least 90% R.H. and are taken from the centre of a prism. This means that the degree of hydration will not strongly differ from the ultimate degree of hydration that could be determined, in case of Portland cement, by Eq. 6 [11]:

$$h_{ultim} = \frac{1.031\ {}^{W}/_{C}}{0.194 + {}^{W}/_{C}} \quad (6)$$

The predicted value is valid for compositions based on CEM I 42,5. In this research, CEM I 52,5 N is used and this type of cement has a higher fineness, which leads to a slightly higher degree of hydration. For these mixtures, a 5% higher value is used (i.e. 0.54 to 0.59) [7]. Fig. 5 gives the variation in capillary porosity for the different mixtures. A similar trend is observed as for the gas permeability. The reference mixture has the smallest value, the lowest porosity and therefore also the lowest capillary porosity.

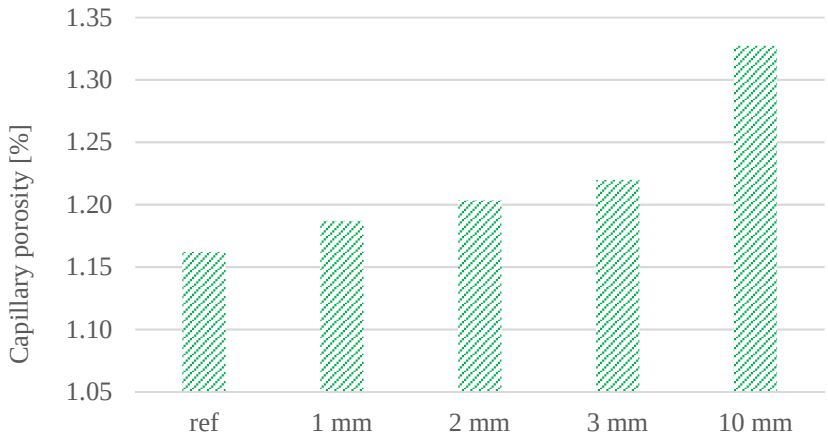


**Fig. 5: Capillary porosity**

Fig. 6 shows the gas permeability for completely dry specimens at inlet pressures of 2, 3 and 4 bar plotted against the calculated capillary porosity. The same correlation could be noticed as for self-compacting concrete (Fig. 7). For the different inlet pressures, a downward shift of the curve is observed when the inlet pressure increases. The correlation coefficient is lower than in case of self-compacting concrete, probably due to the smaller amount of test specimens and the small variation in mixture compositions.

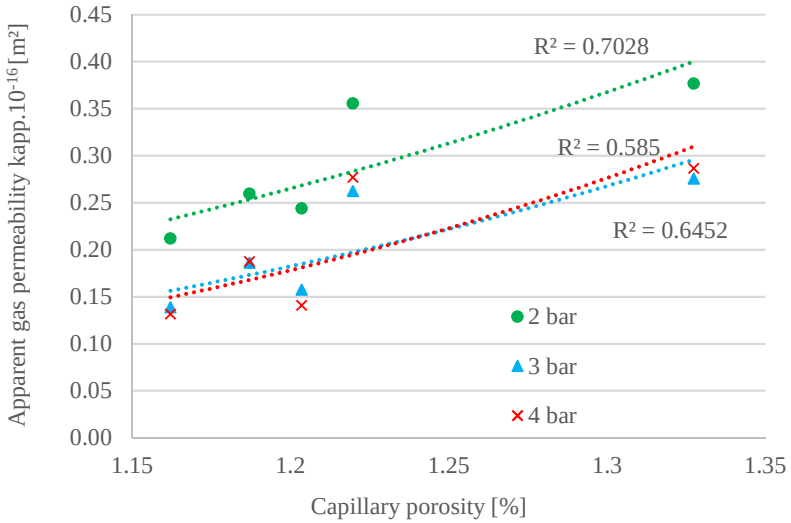


**Fig. 6: Apparent gas permeability versus the calculated capillary porosity in case of UHPC**

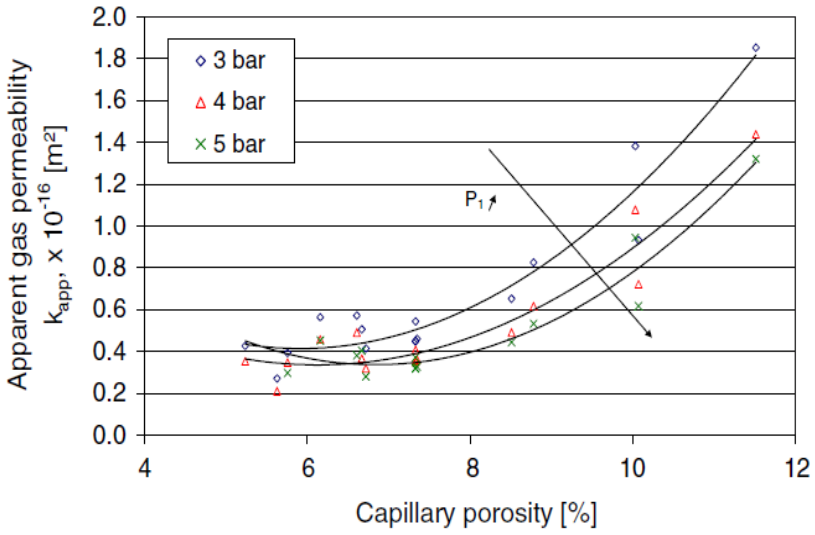


**Fig. 7: Apparent gas permeability at 3 different inlet pressures versus the calculated capillary porosity in case of SCC [7]**

**Compressive strength.** For each mixture, 8 cubes (100 x 100 x 100 mm) are made. The samples are stored in a climate room at 20°C±2°C and a R.H. of more than 90%. Compression tests are performed after 7 and 28 days. During the tests it is important that the pressured area is as flat as possible to avoid stress concentrations. The load is continuously increased until the concrete sample fails. The compressive strength is calculated by dividing the maximum load by the area of the surface the force is exerted on.

Fig. 8 gives an overview of the compressive strength. The volume fraction mortar does not seem to have a large influence on the test results. The strength values on 7 and 28 days are more or less the same. Although a decrease in compressive strength is observed on 7 days, it becomes clear that on 28 days, the compressive strength is on the same level for all the different mixtures. A possible explanations for the differences could be the difference in air content. Other influencing factors could be tiny imperfections in the surface or variation in the dimensions and the flatness of the samples.

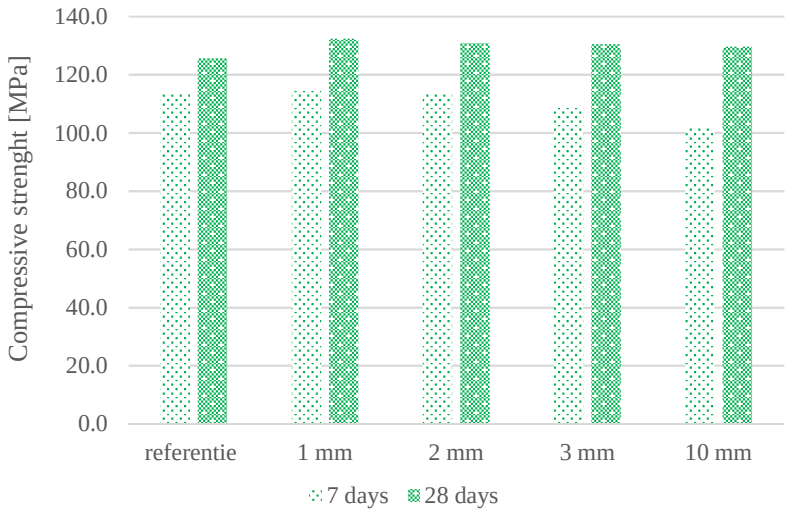


**Fig. 8:** Compressive strength

## Conclusions.

Based on this experimental program, the following conclusions can be obtained:

- ✓ The durability properties of the different UHPC-mixtures decrease when adding a larger amount of paste in order to create different lubrication layer thicknesses;
- ✓ The capillary porosity has been estimated and a rather good correlation has been found with the gas permeability;
- ✓ The increase in paste volume has no influence on the compressive strength of the mixtures. Both on 7 and 28 days, the strength is approximately the same.

## References

[1] Choi, M.S., Y.J. Kim, and S.H. Kwon, *Prediction on pipe flow of pumped concrete based on shear-induced particle migration.* Cement and Concrete Research, 2013. **52**(0): p. 216-224.

[2] Choi, M., et al., *Lubrication layer properties during concrete pumping.* Cement and Concrete Research, 2013. **45**(0): p. 69-78.

[3] Le, H.-D., *Etude de l'effet de la couche limite sur les profils de vitesse du béton pompé*. 2014, University of Ghent and University of Cergy-Pontoise.

[4] Feys, D., *Interactions between rheological properties and pumping of self-compacting concrete*. 2009, University of Ghent.

[5] Kaplan, D., *Pompage des bétons*. 2001: PhD-dissertation, Laboratoire Central des Ponts et Chaussées, Paris.

[6] Feys, D., et al., *Interactions between rheological properties and pumping of concrete*, in *15th International Conference on TRANSPORT AND SEDIMENTATION OF SOLID PARTICLES*. 2011: Wroclaw, Poland.

[7] Boel, V.T.W., K.T.W. Audenaert, and G. De Schutter, *Gas permeability and capillary porosity of self-compacting concrete.* Materials and Structures, 2008. **41**: p. 1283-1290.

[8] Aïssoun, B., S.-D. Hwang, and K. Khayat, *Influence of aggregate characteristics on workability of superworkable concrete.* Materials and Structures, 2015: p. 1-13.

[9] Kropp, J. and H.e. Hilsdorf, *Rilem report 12: performance criteria for concrete durability*.

[10] Marsh, B.K., R.L. Day, and D.G. Bonner, *Pore structure characteristics affecting the permeability of cement paste containing fly ash.* Cement and Concrete Research, 1985. **15**(6): p. 1027-1038.

[11] Van Breugel, K., *Simulation of hydration and formation of structure in cement based materials*, in *PhD thesis*. 1991, TU Delft. p. 321.